

Interaction-induced localization of anomalously-diffracting nonlinear waves

Y. Linzon,¹ Y. Sivan,¹ B. Malomed,² M. Zaezjev,³ R. Morandotti,³ and S. Bar-Ad¹

¹*School of Physics and Astronomy, Faculty of Exact Sciences, Tel-Aviv University, Tel Aviv 69978, Israel*

²*Department of interdisciplinary studies, Faculty of Engineering, Tel-Aviv University, Tel Aviv 69978, Israel*

³*Universite' du Quebec, Institute National de la Recherche Scientifique, Varennes, Quebec J3X 1S2, Canada*

(Dated: October 1, 2018)

We study experimentally the interactions between normal solitons and tilted beams in glass waveguide arrays. We find that as a tilted beam, traversing away from a normally propagating soliton, coincides with the self-defocusing regime of the array, it can be refocused and routed back into any of the intermediate sites due to the interaction, as a function of the initial phase difference. Numerically, distinct parameter regimes exhibiting this behavior of the interaction are identified.

PACS numbers: PACS. 42.65.Tg, 42.65.Jx, 04.30.Nk, 52.35.Mw

Solitary waves in general, and optical solitons in particular, are the most important manifestations of the interplay between nonlinear self-focusing and the diffraction/dispersion, which are inescapable characteristics of linear wave-packet propagation. Periodic structures, such as weakly-coupled waveguide arrays (WGAs) introduce two new important features to this problem. First, they support discrete solitons (DS), which are robust against collapse with increasing input power and propagation length [1, 2]. Second, they allow control over the diffraction properties of tilted beams, giving rise to regions of normal, zero or *anomalous* diffraction for linear excitations [3], and accordingly, regions of self-focusing (SF) or self-defocusing (SDF) for nonlinear excitations [4]. These controllable characteristics not only make such structures favorable candidates for applications in optical switching. They also make optical WGAs a model for a diverse array of classical and quantum systems that have nontrivial dispersion properties and support localized nonlinear modes, from Bose-Einstein condensates in periodic optical lattices [5, 6], to localized lattice vibrations [7] and nonlinear excitations in arrays of mesoscopic-mechanical cantilevers [8].

Recently, there is a growing interest in interactions between co-propagating beams in these WGAs [9, 10], including interactions between spatially-separate solitons [11, 12, 13], as well as between co-propagating solitons and linear waves [14, 15, 16, 17, 18]. In homogeneous Kerr media, mutually coherent in-phase and out-of-phase solitons attract or repel each other, respectively [11]. It was found theoretically [9] and experimentally [14, 15] that the collision between a DS and a weak nondiffracting signal beam can lead to dragging of the blocker soliton towards the weak signal beam. In Ref. [12], Meier *et. al.* have experimentally studied the interaction between two narrow collinear DS in Kerr-nonlinear WGAs fabricated of AlGaAs. It was found that a pair of DSs, separated by 3 sites, are stable (*i.e.* noninteracting) when the relative phase difference between them is around π , and unstable (*i.e.* attractive) when it is close to zero, in accordance with theoretical predictions

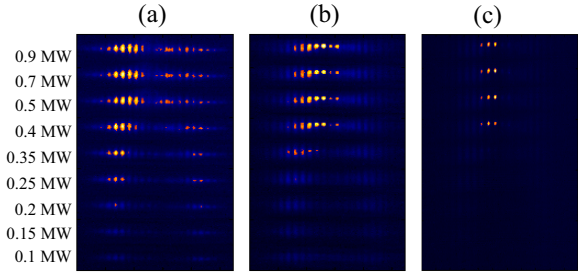


FIG. 1: (Color online) Formation of a single normally injected soliton in the glass waveguide array, for a $40 \mu\text{m}$ wide input beam. The three panels correspond to different imaging conditions, and in each one the input power increases from bottom to top. (a) shows images of the output facet of the sample with the imaging lens adjusted for the laser wavelength. At low powers the discrete-diffraction pattern is observed; at high powers a soliton forms, but is out of focus. (b) The soliton becomes visible at a different focal plane, corresponding to the Raman-shifted wavelength, but its image is saturated. (c) The same image as in (b), with an ND2 filter (X100 attenuation), showing that the soliton is much stronger than the background. Setting (c) is used to study soliton interactions.

[9, 10, 16]. However, interactions involving *tilted* beams, at different diffraction regimes, have never been studied experimentally.

In this paper, we report results for the interaction between a normally-injected soliton (NS) and a nonlinear tilted beam (TB) that propagates *away* from the NS. We find that the characteristics of the interaction are considerably different in the SF and SDF regimes of TB propagation. Specifically, in the SDF regime we demonstrate for the first time that it is possible to *restore* self-focusing to the TB, and to redirect it into any of the intermediate sites, by varying the relative phase difference.

We use a WGA fabricated of silica glass, as in Ref. [19], with the periodicity $d = 12 \mu\text{m}$ and coupling constant $C = 0.23 \text{ mm}^{-1}$. The sample is 13 mm long, corresponding to 1.8 coupling lengths. As the Kerr coefficient in glass is ~ 500 times smaller than in AlGaAs [11], shorter pulses with higher peak powers are required to

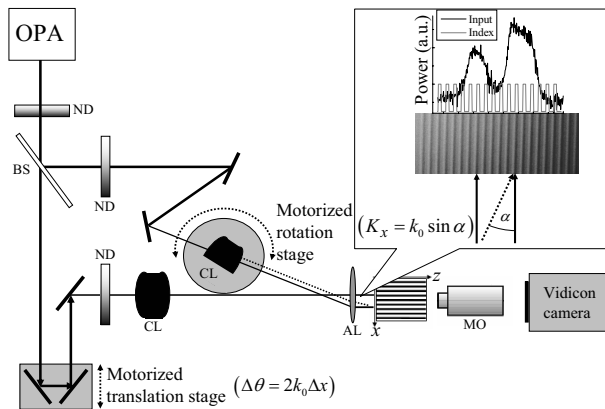


FIG. 2: Experimental setup. OPA - optical parametric amplifier, BS - beam splitter, ND - neutral density filter, CL - cylindrical lens, AL - aspherical lens, MO - microscope objective. Inset: Lateral intensity profile of the input beams. The normal beam excites $\simeq 3$ -4 sites, while the tilted beam excites $\simeq 4$ -5 sites. The excitation parameters, $\Delta\theta$ and K_x , described in the text, are determined from applied translations and rotations, respectively, using the free-space wavenumber $k_0 = 2\pi/\lambda_0$.

generate nonlinear effects. Importantly, the lowest-order nonlinear loss mechanism in glass is six-photon absorption, which has an extremely low probability amplitude. DSs in glass WGAs, including TBs, are therefore sustained at high powers without breakup [19], allowing a broader range of powers and tilts to be explored. Glass is also characterized by strong stimulated Raman scattering, which expresses itself as self frequency-shift of the soliton's spectrum to longer wavelengths [18]. The formation of a soliton is therefore accompanied by a change of the focusing plane, due to the chromatic aberration of the output microscope objective lens. This sudden change of focus enables us to distinguish between strong solitary features and the linear background without explicit spectral measurements, as demonstrated in Fig. 1.

The experimental setup for the 2-beam experiment is sketched in Fig. 2. A train of 70-fs pulses at $\lambda_0=1.52 \mu\text{m}$, with ≤ 20 MW peak power, was split into two identical beams. The normally injected beam forming the NS was given an adjustable phase delay $\Delta\theta$ using a variable delay stage, and shaped using a cylindrical lens. The second beam passed through a rotating cylindrical lens that moved the beam on the aspherical coupling lens, and thus changed its angle of incidence α at the input facet of the sample. This angle determines the transverse wavenumber K_x and thus the phase difference between adjacent sites in the TB excitation. Both beams were coupled into the sample through the same aspherical lens, which has a large numerical aperture (0.68 NA) and is optimized for the operating wavelength. A unique feature of this setup is the large clear aperture of the coupling lens, which in combination with its small focal

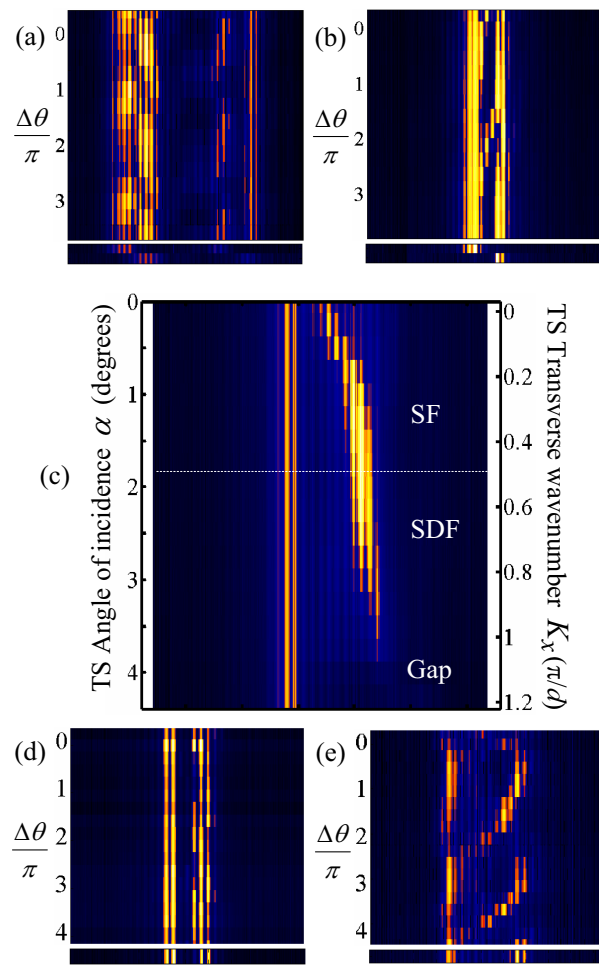


FIG. 3: (Color online) (a),(b) Output profiles as a function of the phase difference, with both beams at normal incidence. The input powers are (a) 0.15 MW, and (b) 0.7 MW (Linear and soliton regimes, respectively). (c) The output profiles of *noninteracting* 0.7 MW beams as a function of the TB tilt (data obtained with a very large time delay between the pulses). (d),(e) Interactions of 0.7 MW beams as a function of the phase difference for the tilt angles of (d) 0.6° ($K_x = 0.17\pi/d$), and (e) 3° ($K_x = 0.84\pi/d$). The bottom parts in (a),(b),(d) and (e) show the output in the absence of interaction.

length, results in a wide range of accessible incidence angles for the tilted beam, while maintaining paraxiality conditions and good coupling efficiency. The edge of the first Brillouin zone for this sample is attained at an incidence angle of $\alpha = \arcsin(\lambda_0/2d) = 3.6^\circ$. In order to have sufficient resolution in K_x , that allows probing of the different diffraction regimes for the TB, the lateral width of the input TB had to be larger than $\sim 30 \mu\text{m}$. The combined input intensity profile for the two beams is shown in the inset of Fig. 2. The TB input profile did not vary under relevant tilts.

Experimental results are shown in Fig. 3. Panels (a),(b) show the results obtained when the two beams

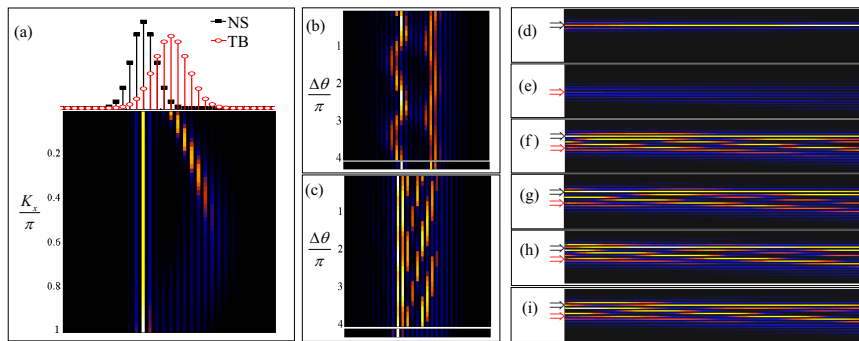


FIG. 4: (Color online) Results of numerical simulations. (a) Top: the amplitude distribution in the input, $|\Phi_n(0)|$. Bottom: output intensity distributions as a function of the tilt K_x for noninteracting beams (*i.e.*, superposition of individual solutions). (b),(c) Output intensity distribution as a function of the phase difference for: (b) $K_x = 0.24\pi$ and (c) $K_x = 0.9\pi$. (d)-(i) Propagation maps of the intensity distribution as a function of z for $0 < z < 13$ mm and $K_x = 0.9\pi$: (d) NS without TB; (e) TB without NS; (f)-(i) both beams present, with the relative initial phase differences: (f) 0, (g) $\pi/2$, (h) π , and (i) $3\pi/2$.

are at normal incidence. At low input powers (a), linear interference fringes are superimposed on the superposition of the two overlapping discrete-diffraction patterns. It was found that the slope of the fringes exactly coincided with the phase slope imposed by the translation motor. At high input powers (b), the anticipated nonlinear instability around $\Delta\theta = 2\pi$, which partially diverts the beams into intermediate sites, is observed [12].

As tilts are imposed on the right DS (Fig. 3(c)), it is routed aside. As expected, the sideways shift of the beam increases in the SF regime, and decreases again in the SDF regime, where the beam becomes delocalized (The data in Fig. 3(c) was obtained with a very large time delay between the pulses, which inhibits the interaction). Panels (d) and (e) of Fig. 3 show examples of interacting NS and TB in the SF and SDF regimes of the TB, respectively. For small tilts that correspond to a TB in the SF regime (Fig. 3(d)), the observed attractive instability near 2π phase multiples is less pronounced compared to the collinear excitation (Fig. 3(b)). This may be expected due to the decreasing overlap of the two fields as the TB is routed aside. However, when the tilt angle is in the SDF regime of the TB (Fig. 3(e)), the instability is extended for phase differences far beyond a vicinity of 2π . Remarkably, the TB can be routed as a localized DS into any of the intermediate sites, with the appropriate phase setting, while the NS is partially annihilated. Evidently, the WGA favors interaction when one of the beams propagates in the SF regime and the other one in the SDF regime, as demonstrated by the extended range of phases exhibiting interaction dynamics.

In order to gain better understanding of the interaction dynamics, we solved the one-dimensional discrete nonlinear Schrödinger equation in dimensionless form [1, 20],

$$i \frac{d\Phi_n}{dz} + h^{-2}(\Phi_{n+1} + \Phi_{n-1} - 2\Phi_n) + |\Phi_n|^2 \Phi_n = 0, \quad (1)$$

on a grid of 101 sites; $h^{-2} = Z_{NL}C$, the ratio be-

tween the characteristic nonlinear length Z_{NL} and the diffraction length $Z_D = 1/C$, is a single parameter characterizing the sample. The input is taken as two Gaussians centered at waveguide numbers $n_{c1} = 51$ and $n_{c2} = 55$,

$$\Phi_n(0) = \frac{A_{NS}}{\sqrt{P^*}} \exp\left(-\frac{(n - n_{c1})^2}{(w_1)^2}\right) + \frac{A_{TB}}{\sqrt{P^*}} \exp\left(-\frac{(n - n_{c2})^2}{(w_2)^2} + iK_x n + i\Delta\theta\right), \quad (2)$$

where P^* is the characteristic soliton power that defines Z_{NL} [20]. We took $P^* = 0.5$ MW. This value and the other experimental parameters (*e.g.* the diffraction length, mode area, and Kerr coefficient) yield $h^{-2} = 4.9 \times 10^{-3}$. The input widths, $w_1 = 2.5$ and $w_2 = 3.5$, correspond to the experimental conditions. Finally, in these units the first band of linear waves corresponds to $0 < K_x < \pi$.

We have found that, to reproduce the propagation dynamics observed in the experiment, two conditions must hold regarding the excitation amplitudes. First, the TB amplitude, for the above input width, must be $45 < A_{TB} < 60$. For higher amplitudes (with $A_{NS} = 0$) the steering of the TB to nearby sites in the SF region is suppressed, and the soliton instead becomes trapped in one waveguide [10, 21]. Simultaneously, it becomes unstable under small variations of the tilt. The second condition pertains to the NS. While the excitation amplitude must be $40 < A_{NS} < 90$ for a NS to form by itself (*i.e.* with $A_{TB} = 0$), we have found that it must be comparable to the TB amplitude when the two excitations are sent together with the initial condition (2). Otherwise, the TB vanishes during the propagation, with only a small effect on the NS. In addition to the above constraints on the excitation amplitudes, we have also found that the balance between the strength of diffraction and nonlinearity must be in favor of the nonlinearity, in the

form of a small h^{-2} parameter, to avoid breakup of the TB into filaments due to modulational instability [22]. Indeed, all of the above conditions were fulfilled in our experiment.

Results of the numerical simulations are shown in Fig. 4, for $A_{\text{NS}} = 48$ and $A_{\text{TB}} = 40$. Figure 4(a) shows the amplitude profile of the input beam and the output intensity distribution for individual (non-interacting) beams, as a function of the TB tilt. Figures 4(b) and 4(c) show the output intensity distribution as a function of the initial phase difference, for a TB that is SF and SDF, respectively. The calculated results are in good qualitative agreement with the experimental data displayed in Fig. 3. In particular, Fig. 4(c) indeed shows routing of a relocalized TB to nearby sites, which changes gradually over the entire range of the phase difference, $0 < \Delta\theta < 2\pi$. The propagation maps as a function of z , panels (d)-(i), demonstrate how the NS is re-phasing the otherwise defocusing TB to form a localized soliton. The initial re-phasing generates a DS around one of the intermediate sites, which then periodically hops outwards. While the initial site in which the DS forms is a function of $\Delta\theta$, the hopping period is always the same for a given K_x , corresponding to a constant propagation angle. The good agreement with the experimental data suggests that the spectral and temporal dynamics are not crucial for the understanding of the observed interactions.

In conclusion, we have studied experimentally the interactions among two non-collinear discrete solitons in glass waveguide arrays. We have demonstrated for the first time that a tilted beam (TB) launched in a self-defocusing direction, while deviating away from its normally propagating counterpart (NS), can be re-localized and routed into any intermediate site by the nonlinear interaction with the NS. The routing is controlled by the initial phase difference between the solitons. In simulations, this behavior was reproduced under several conditions, in which (i) the nonlinear length is considerably smaller than the diffraction length; (ii) the NS and TB have comparable input amplitudes; and (iii) the TB input amplitude is moderate, to enable soliton steering and to avoid its trapping and instability. When two on-site excitations exist simultaneously, $\Phi_n = A + B$, the nonlinear Kerr term in the coupled equations (1) acts as a non-trivial interference term $|\Phi_n|^2\Phi_n = (|A|^2 + |B|^2 + 2|A||B|\sin\Delta\theta)(A + B)$, and a new propagation mode that is in balance with the weak inter-site coupling is obtained. Under the above conditions for the initial collective excitation, this mode favors localization of the initially SDF TB, which can indeed be controlled with the initial phase difference as a single parameter. The result is a unique recapturing of a defocusing beam into a soliton, which should have analogs in many other physical systems that have nontrivial dispersion properties and support localized nonlinear modes. In addition, the interaction that we observe has potential applications in

all-optical switching devices.

This work was supported by the Israel Science Foundation through an Excellence-Center grant No. 8006/03 and contract No. 0900017, and by NSERC in Canada. We thank V. Fleurov and S. Flach for enlightening discussions. Y.L. appreciates hospitality of Université du Québec during his stay.

-
- [1] D. N. Christodoulides and R. I. Joseph, *Opt. Lett.* **13**, 794 (1988).
 - [2] H. S. Eisenberg, Y. Silberberg, R. Morandotti, A. R. Boyd, and J. S. Aitchison, *Phys. Rev. Lett.* **81**, 3383 (1998).
 - [3] H. S. Eisenberg, Y. Silberberg, R. Morandotti, and J. S. Aitchison, *Phys. Rev. Lett.* **85**, 1863 (2000).
 - [4] R. Morandotti, H. S. Eisenberg, Y. Silberberg, M. Sorel, and J. S. Aitchison, *Phys. Rev. Lett.* **86**, 3296 (2001).
 - [5] E. A. Ostrovskaya and Y. S. Kivshar, *Phys. Rev. Lett.* **92**, 180405 (2004).
 - [6] A. Gubesky, B. A. Malomed, and I. M. Merhasin, *Phys. Rev. A* **73**, 023607 (2006).
 - [7] S. Flach and C. R. Willis, *Phys. Rep.* **295**, 181 (1998).
 - [8] M. Sato, B. E. Hubbard, and A. J. Sievers, *Rev. Mod. Phys.* **78**, 137 (2006).
 - [9] D. N. Christodoulides and E. D. Eugenieva, *Phys. Rev. Lett.* **87**, 233901 (2001).
 - [10] A. B. Aceves, C. DeAngelis, T. Peschel, R. Muschall, F. Lederer, S. Trillo and S. Wabnitz, *Phys. Rev. E* **53**, 1172 (1996).
 - [11] G. I. Stegeman and M. Segev, *Science* **286**, 1518 (1999).
 - [12] J. Meier, G. I. Stegeman, Y. Silberberg, R. Morandotti, and J. S. Aitchison, *Phys. Rev. Lett.* **93**, 093903 (2004); J. Meier, G. I. Stegeman, D. N. Christodoulides, R. Morandotti, M. Sorel, H. Yang, G. Salamo, J. S. Aitchison, and Y. Silberberg, *Opt. Exp.* **13**, 1797 (2005).
 - [13] I. E. Papacharalampous, P. G. Kevrekidis, B. A. Malomed, and D. J. Frantzeskakis, *Phys. Rev. E* **68**, 046604 (2003).
 - [14] J. Meier, G. I. Stegeman, D. N. Christodoulides, R. Morandotti, G. Salamo, H. Yang, M. Sorel, Y. Silberberg, and J. S. Aitchison, *Opt. Lett.* **30**, 1027 (2005).
 - [15] J. Meier, G. I. Stegeman, D. N. Christodoulides, Y. Silberberg, R. Morandotti, H. Yang, G. Salamo, M. Sorel, and J. S. Aitchison, *Opt. Lett.* **30**, 3174 (2005).
 - [16] T. Kapitula, P. G. Kevrekidis, and B. A. Malomed, *Phys. Rev. E* **63**, 036604 (2001).
 - [17] S. Flach, V. Fleurov, A. V. Gorbach, and A. E. Miroshnichenko, *Phys. Rev. Lett.* **95**, 023901 (2005).
 - [18] A. Efimov, A. V. Yulin, D. V. Skryabin, J. C. Knight, N. Joly, F. G. Omenetto, A. J. Taylor, and P. Russell, *Phys. Rev. Lett.* **95**, 213902 (2005).
 - [19] D. Cheskis, S. Bar-Ad, R. Morandotti, J. S. Aitchison, H. S. Eisenberg, Y. Silberberg, and D. Ross, *Phys. Rev. Lett.* **91**, 223901 (2003).
 - [20] M. J. Albowitz and Z. H. Musslimani, *Physica D* **184**, 276 (2003).
 - [21] O. Bang and P. D. Miller, *Opt. Lett.* **21**, 1105 (1996).
 - [22] J. Meier, G. I. Stegeman, D. N. Christodoulides, Y. Silberberg, R. Morandotti, H. Yang, G. Salamo, M. Sorel,

and J. S. Aitchison, Phys. Rev. Lett. **92**, 163902 (2004).